

## Supporting Information

### Towards the Fastest Kinetics and Highest Uptake of Post- Functionalized UiO-66 for Hg<sup>2+</sup> Removal from Water

Iris Tsz Yan Lam<sup>1</sup>, Yufei Yuan<sup>1</sup>, Ki-Taek Bang<sup>1</sup>, Seon-Jin Choi<sup>2</sup>, Dong-Myeong Shin<sup>3</sup>, Dong Lu<sup>4</sup>,  
and Yoonseob Kim<sup>1,\*</sup>

<sup>1</sup>Department of Chemical and Biological Engineering, The Hong Kong University of Science and  
Technology, Hong Kong SAR, China

<sup>2</sup>Division of Materials of Science and Engineering, Hanyang University, Seoul 04763, Republic of  
Korea

<sup>3</sup>Department of Mechanical Engineering, The University of Hong Kong, Pokfulam Road, Hong  
Kong SAR, China

<sup>4</sup>Centre for Engineering Materials and Reliability, Guangzhou HKUST Fok Ying Tung Research  
Institute, Guangzhou, 511458, China

\*To whom correspondence should be addressed: yoonseobkim@ust.hk

#### Chemicals

Zirconium(IV) chloride (Sigma-Aldrich, ACS reagent, 99.5%), 2-aminoterephthalic acid  
(Energy Chemical, ACS reagent, 98%), N,N-dimethylformamide (RCI Labscan, AR., 99.9%),  
dichloromethane (Scharlau, ACS reagent, 99.9%) formic acid (Scharlau, ACS reagent, 98%–  
100%), nitric acid (Fisher, ACS reagent, 68–70%), 3,3'-disulfanediyldipropanoic acid (Macklin,  
ACS reagent, 99%), N,N'-Diisopropylcarbodiimide (Energy Chemical, ACS reagent, 98%),  
Dithiothreitol (Aladdin, ACS reagent, 97%), caesium fluoride (3A, ACS reagent, 99.5%),  
mercury(II) sulfate (Riedel-de Haën, ACS reagent, 98%), cadmium nitrate tetrahydrate (Sigma-  
Aldrich, ACS reagent, 98%), cobalt(II) nitrate hexahydrate (Acros Organics, ACS reagent, 98%),

copper(II) nitrate hemi(pentahydrate) (Sigma-Aldrich, ACS reagent, 98%), zinc nitrate hexahydrate (Sigma-Aldrich, reagent grade, 98%), nickel(II) nitrate hexahydrate (Sigma-Aldrich, ACS reagent, 98.5%) lead(II) nitrate (Sigma-Aldrich, ACS reagent, 99.0%), chromium(III) nitrate nonahydrate (Sigma-Aldrich, ACS reagent, 100%), iron(III) nitrate nonahydrate (Sigma-Aldrich, ACS reagent, 98%) were used without further purification. 1,000 ppm arsenic stock solution was purchased from High-Purity Standards. Deionized water (18.2 M  $\Omega$  cm) was used. The concentration of HNO<sub>3</sub> in all the heavy metal ion stock solutions is 5%.

### **General testing and characterization methods**

The morphologies of the as-synthesized materials were performed on an SEM (JSM-7800). The samples were gold coated before SEM measurement. The crystal structure was examined on an analytical X-ray diffractometer (Cu K $\alpha$  radiation  $\lambda = 1.54056 \text{ \AA}$ ). Nitrogen adsorption/desorption isotherms were recorded with a Micromeritics 3Flex apparatus at 77 K to determine the Brunauer-Emmet-Teller (BET) surface area. Prior to measuring nitrogen isotherms, the samples were activated by heating to 120°C for 3 hours under vacuum at a pressure of 100 mtorr. The Fourier transform infrared (FTIR) spectra were recorded by a Thermo Fisher Nicolet IS50. The X-ray photoelectron spectroscopy (XPS) was measured by a Kratos Axis Ultra DLD multi-technique surface analysis system. TGA was measured from 25°C to 700°C with a heating rate of 5°C min<sup>-1</sup>. The chemical bonds of the MOFs were measured using Bruker 400 MHz <sup>1</sup>H NMR. Contact angle meter Biolin was used for contact angle measurement.

## Synthetic Procedures

### 1. Synthesis of UiO-66-NH<sub>2</sub> MOFs

UiO-66-NH<sub>2</sub> MOFs were prepared by solvothermal strategy.<sup>1</sup> Zirconium(IV) chloride (1.280 g, 5.4926 mmol) and 2-aminoterephthalic acid (0.995 g, 5.4926 mmol) were added in 200 mL of DMF in a 350-mL screw-capped glass jar, sonicated until fully dissolved. Formic acid (50 mL) was added to the solution, then the glass jar was heated in an oven at 100°C for 24 h for a solvothermal reaction. After cooling, the precipitate was washed by centrifugation with DMF and acetone, each for 3 days, and three times per day. The MOFs were dried overnight in the oven at 100°C before characterization.

### 2. Post-functionalization of UiO-66-NH<sub>2</sub>

UiO-66-A.T. were synthesized with some modifications.<sup>2</sup> 3,3'-Disulfanediylidipropionic acid (210.3 mg, 1.00 mmol), and diisopropylcarbodiimide (162  $\mu$ L, 1.03 mmol), UiO-66-NH<sub>2</sub> (10.99 mg, contains approximately 0.2 mmol NH<sub>2</sub> functional groups) were added after added to 40 mL of chloroform, heated in reflux for 7 hours. The sample was filtered and washed with acetone. 10.5 mg of the product and 1 g of dithiothreitol were added into 27 mL of ethanol and stirred at room temperature for 1 day. The sample was filtered and washed with ethanol. The powder was dried overnight in the oven at 100°C before characterization. NMR analysis was performed on digested samples. UiO-66-A.T. was acid digested in a mixture of 0.4 mL DMSO-d<sub>6</sub> and 0.2 mL of CsF in D<sub>2</sub>O.

A thiol-disulfide exchange reaction took place to form a stable six-membered ring with an internal disulfide bond. The crosslinking reaction was carried out at five different reaction

conditions (Table S3),<sup>2</sup> chloroform in reflux for 7 hours demonstrated the optimized sulfur mass percentage of 9.56%.

## NMR Spectra

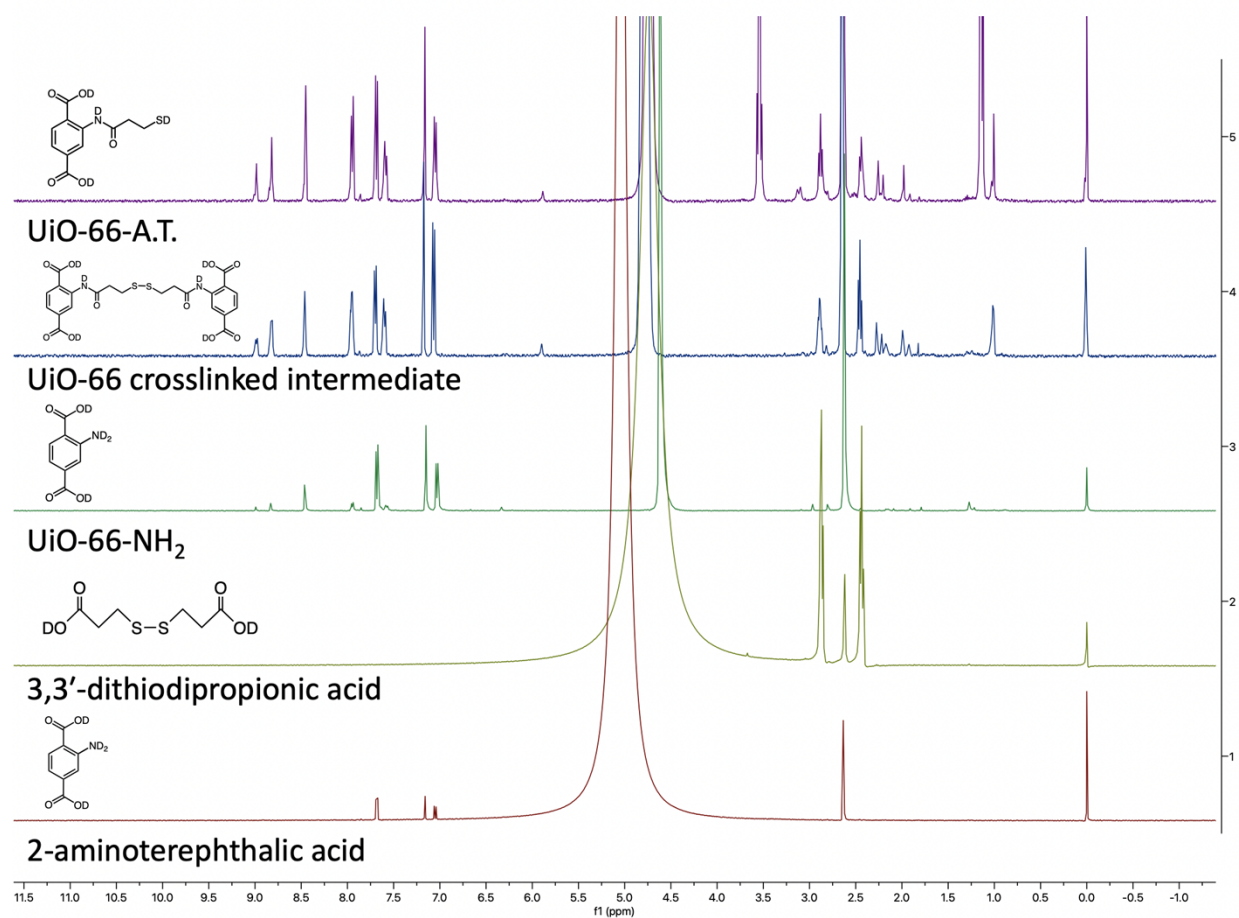


**Figure S1a.** Stacked <sup>1</sup>H NMR spectra of the digested UiO-66-A.T.

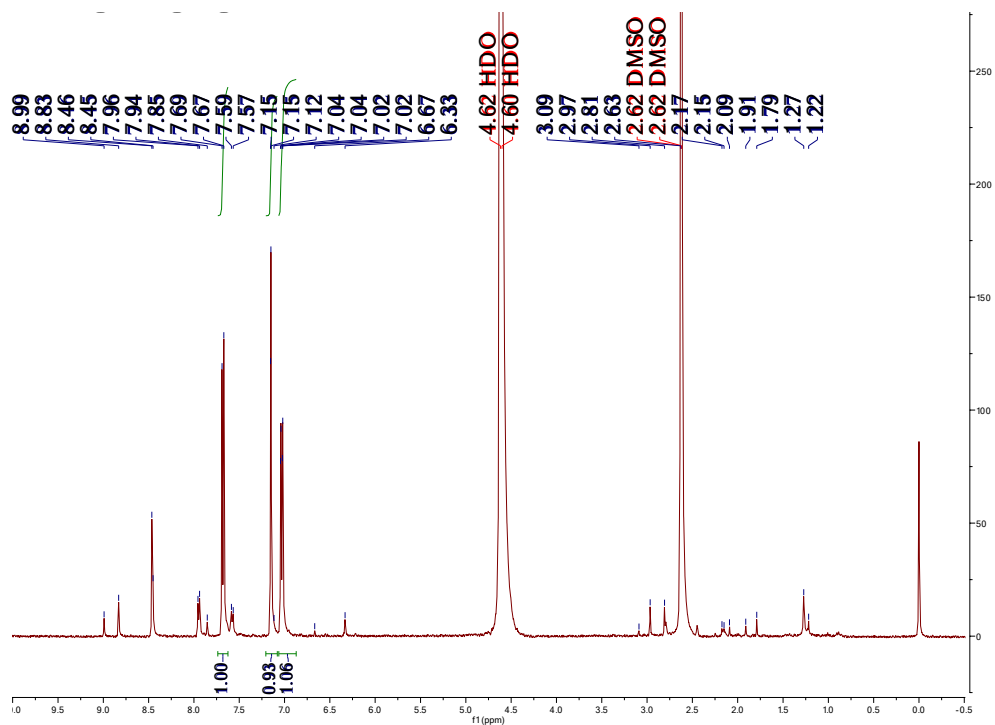


**Figure S1b.**  $^1\text{H}$  NMR spectra of the digested UiO-66-NH<sub>2</sub>

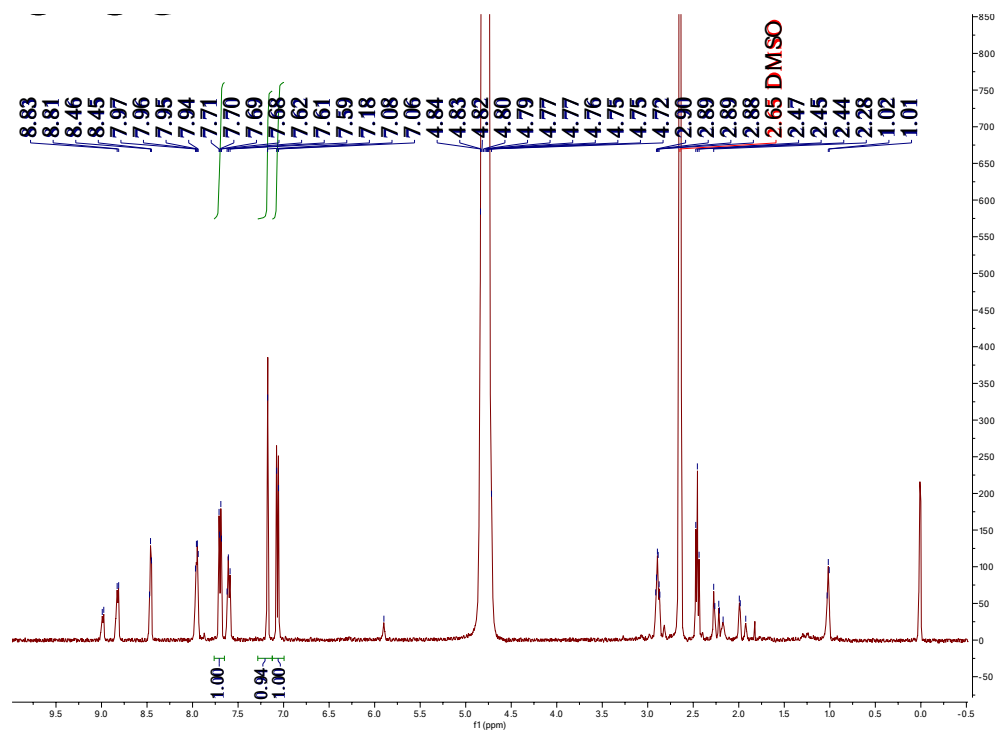


**Figure S1c.**  $^1\text{H}$  NMR spectra of the digested UiO-66 crosslinked intermediate before S-S cleavage.

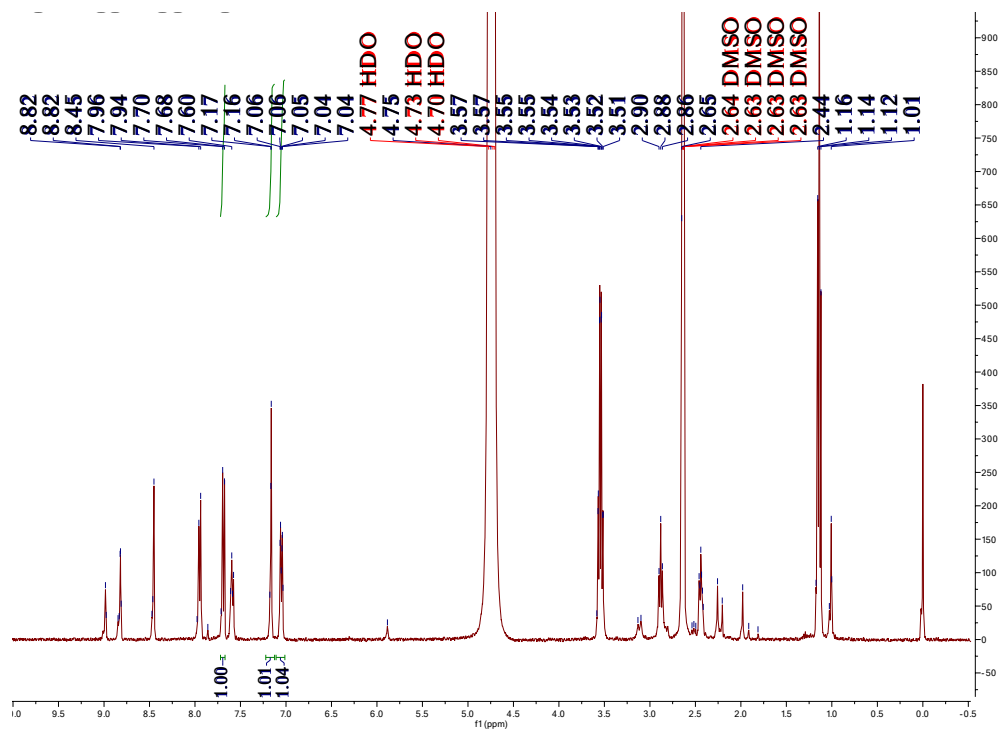


**Figure S1d.** <sup>1</sup>H NMR spectra of the digested UiO-66-A.T.

**Figure S1.** Digested NMR of the MOFs.

## Other data

The adsorption capacity of heavy metal ions was calculated according to Equation S1:

$$q_e = (C_0 - C_e) \frac{V}{m} \text{ (Eq. S1)}$$

where  $q_e$  (in  $\text{mg g}^{-1}$ ) is the amount of heavy metal ion adsorbed at equilibrium,  $C_0$  and  $C_e$  (in  $\text{mg L}^{-1}$ ) are the initial and equilibrium metal ion concentration, respectively.  $V$  (in L) is the volume of the metal solution, and  $m$  (in g) is the mass of the adsorbent used.

Freundlich isotherm model (Equation S2) and Langmuir isotherm model (Equation S3) are used to analyze the adsorption kinetics of  $\text{Hg}^{2+}$  (Fig. S9c, 3f inset).

$$\ln q_e = \ln K_f + \frac{1}{n} \ln C_e \text{ (Eq. S2)}$$

$$\frac{C_e}{q_e} = \frac{C_e}{q_{\max}} + \frac{1}{q_{\max} b} \text{ (Eq. S3)}$$

where  $q_{\max}$  is the maximum adsorption capacity,  $K_f$  and  $b$  are bare Freundlich constant and Langmuir constant, respectively, and  $n$  is the dimensionless exponent of Freundlich equation.

**Table S1. Mass percentage before and after deprotection obtained by XPS.**

Elements	mass %	
	Before deprotection	After deprotection
C	35.65	38.03
N	3.22	3.64
S	11.22	6.24
O	27.25	27.16
Zr	22.67	24.93

**Table S2. Hg<sup>2+</sup> adsorption performance of different adsorbents and post-functionalized UiO-66-NH<sub>2</sub>**

Adsorbent	Adsorption		References
	Capacity (mg g <sup>-1</sup> )	Rate Constant (g mg <sup>-1</sup> min <sup>-1</sup> )	
Activated Carbon	2	0.0129	3
Zeolite	8	0.0008	4
Biomass	20	0.0280	5
PTMS-functionalized Silica Gel	132	0.0001	6
Thiol functionalized silica nano hollow sphere	210	0.0002	7
UiO-66	59	—	8
UiO-66-NH <sub>2</sub>	103	—	9



UiO-66-NH <sub>2</sub>	113	–	10
UiO-66-NH <sub>2</sub>	145	–	8
UiO-66-NH <sub>2</sub>	208	0.0051	This work
UiO-66-SH	110	0.0114	11
Zr-DMBD	172	0.0050	12
Zr-L1	193	–	13
Zr-L3	245	–	
NSU66	265	–	14
Zr-L2	275	–	13
Zr-L4	322	–	
UiO-66-AHMT	328 (600 ppm stock solution)	0.0005	9
PCN-224-ALA(O)	344	–	15
Cys-UiO-66	350	0.0001	10
UiO-66-EDTA	372	0.0025	16
ZrOMTP	403	–	17
PCN-222-MAA(O)	509	–	15
UiO-66-QU	556 (600 ppm stock solution)	0.0050	18
UiO-66-IT	580 (1500 ppm stock solution)	0.0032	19
Zr-MOF-NAC	594 (800 ppm stock solution)	0.0070	20

UiO-66-DMTD	671 (700 ppm stock solution)	0.0012	8
UiO-66-A.T.	691	0.2823	This work

**Table S3. Sulfur mass percentage according to different reaction conditions**

Conditions	Attempt	Sulfur mass %	Average sulfur mass %
DMF, rt, 2 days	1	3.88	3.86
	2	3.83	
DMF, 50°C, 7 hours	1	3.01	3.32
	2	3.63	
DCM, rt, 2 days	1	6.24	5.36
	2	4.47	
DCM, reflux, 7h	1	5.03	4.85
	2	4.66	
Chloroform, reflux, 7h	1	7.89	<b>9.56</b>
	2	11.22	

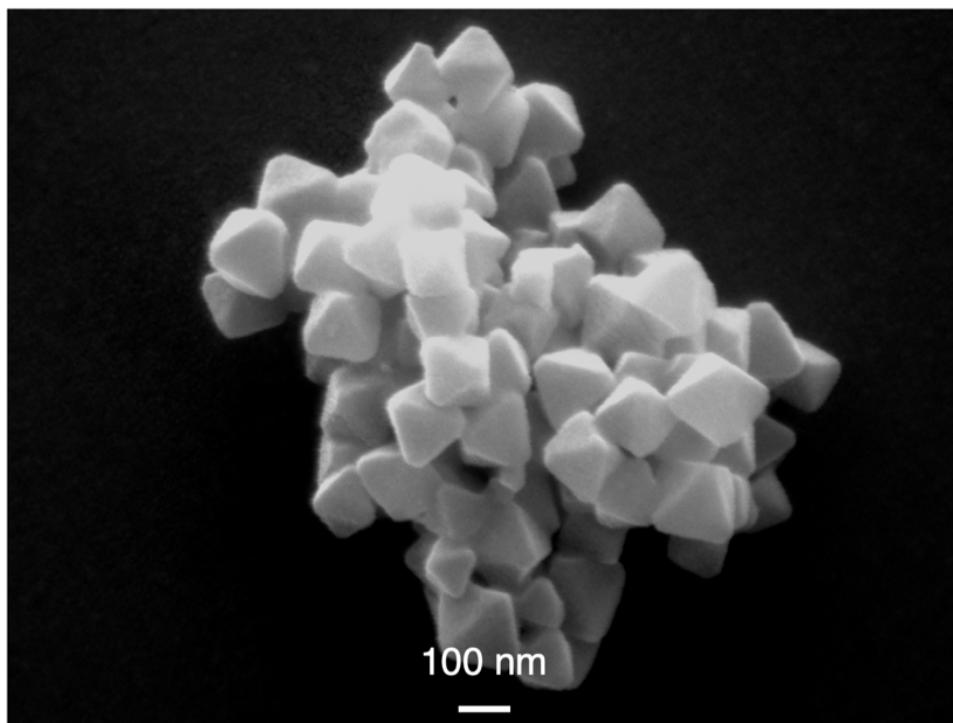


**Figure S2.** Scanning electron microscopy image of UiO-66-A.T.

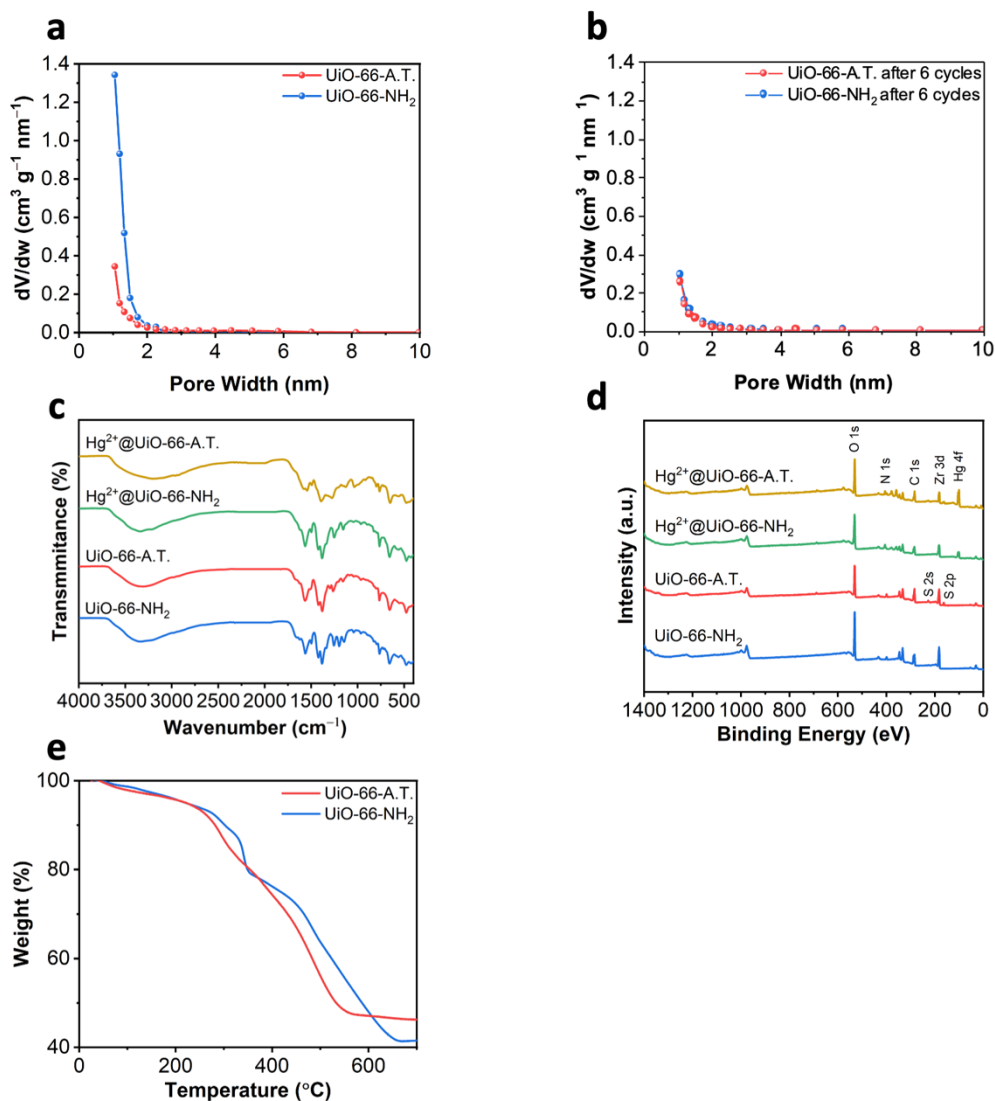


**Figure S3. Characterization of UiO-66-MOFs.** **a**, Barrett-Joyner-Halenda (BJH) pore size distributions of UiO-66-A.T. and UiO-66-NH<sub>2</sub>. **b**, BJH pore size distributions of UiO-66-A.T. and UiO-66-NH<sub>2</sub> after 6 cycles. **c**, FTIR spectra of UiO-66-A.T., UiO-66-NH<sub>2</sub>, Hg<sup>2+</sup> adsorbed UiO-66-A.T., Hg<sup>2+</sup> adsorbed UiO-66-NH<sub>2</sub>. **d**, XPS spectra of UiO-66-A.T., UiO-66-NH<sub>2</sub>, Hg<sup>2+</sup> adsorbed UiO-66-A.T., Hg<sup>2+</sup> adsorbed UiO-66-NH<sub>2</sub>. **e**, TGA of UiO-66-A.T. and UiO-66-NH<sub>2</sub>.

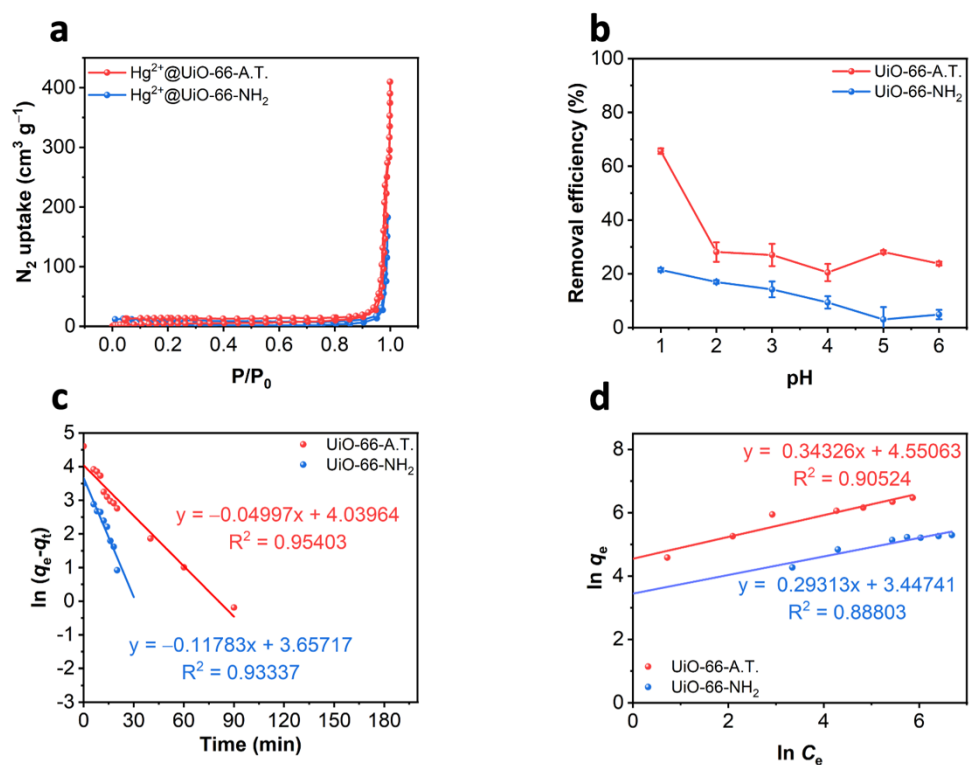


**Figure S4. Adsorption performance of UiO-66-MOFs. a**, Nitrogen adsorption isotherms of UiO-66-A.T. and UiO-66-NH<sub>2</sub> after Hg<sup>2+</sup> adsorption. **b**, Removal efficiency at different pH conditions. **c**, Pseudo-first-order fitting. **d**, Linear regression by fitting the equilibrium adsorption data with Freundlich model.

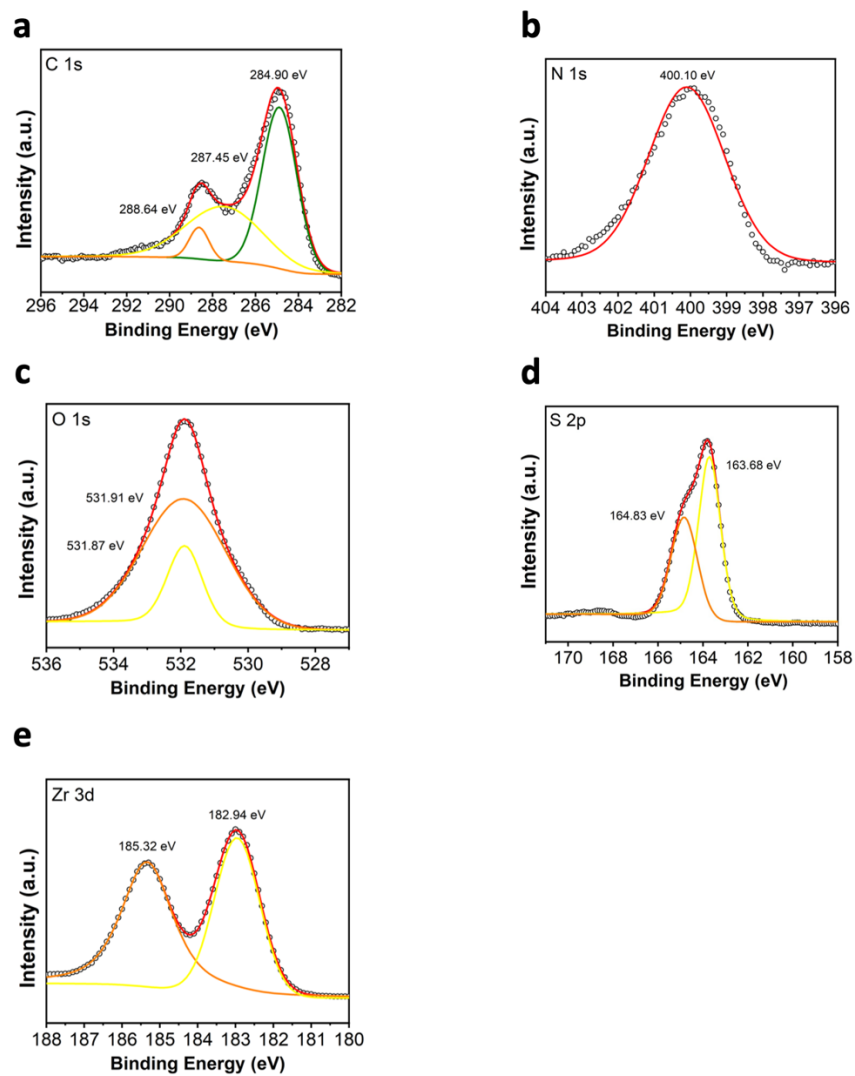


**Figure S5.** XPS spectra of UiO-66-A.T. **a**, C 1s spectra. **b**, N 1s spectra. **c**, O 1s spectra. **d**, S 2p spectra. **e**, Zr 3d spectra.

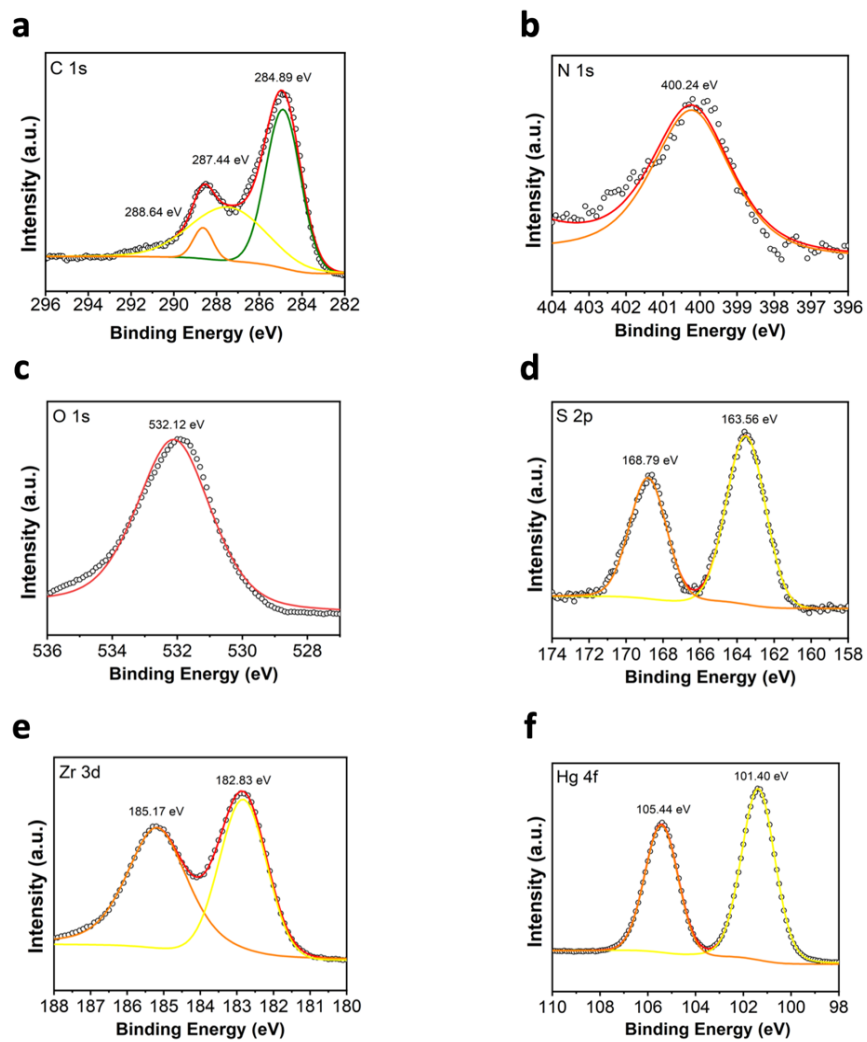


**Figure S6.** XPS spectra of  $\text{Hg}^{2+}@UiO-66\text{-A.T.}$  **a**, C 1s spectra. **b**, N 1s spectra. **c**, O 1s spectra. **d**, S 2p spectra. **e**, Zr 3d spectra. **f**, Hg 4f spectra.

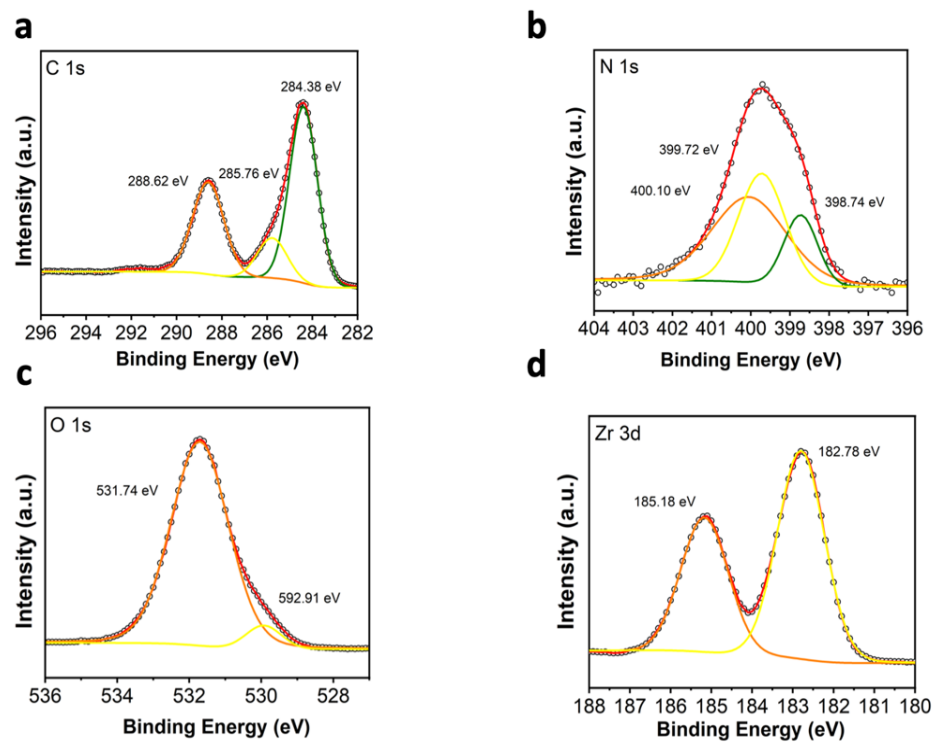


**Figure S7. XPS spectra of UiO-66-NH<sub>2</sub>. a, C 1s spectra. b, N 1s spectra. c, O 1s spectra. d, Zr 3d spectra.**



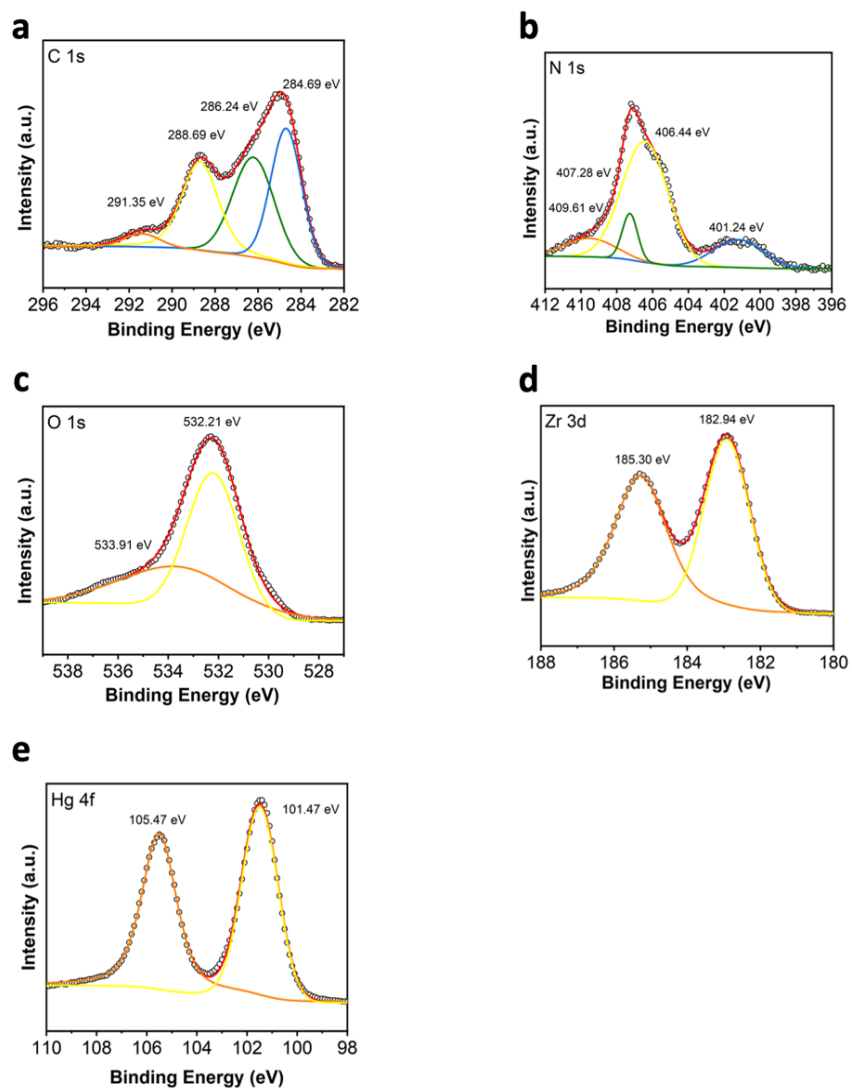


**Figure S8.** XPS spectra of  $\text{Hg}^{2+}@\text{UiO-66-NH}_2$ . **a**, C 1s spectra. **b**, N 1s spectra. **c**, O 1s spectra. **d**, Zr 3d spectra. **e**, Hg 4f spectra.

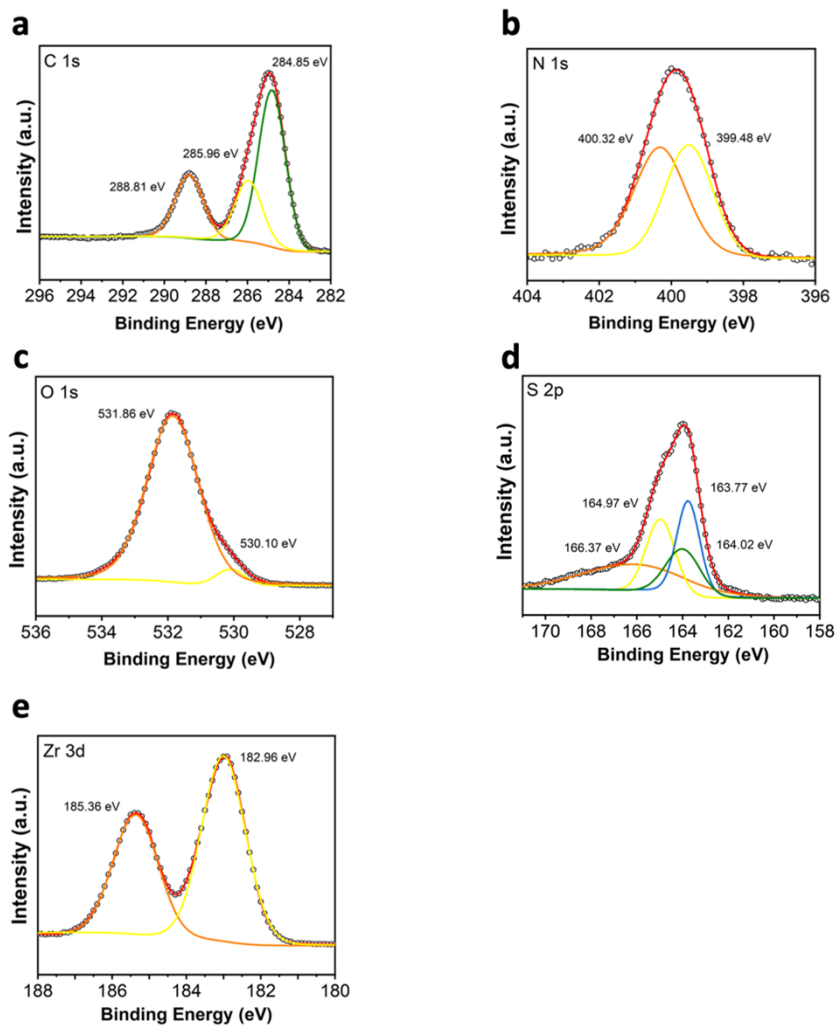


**Figure S9.** XPS spectra of UiO-66 crosslinked intermediate. **a**, C 1s spectra. **b**, N 1s spectra. **c**, O 1s spectra. **d**, S 2p spectra. **e**, Zr 3d spectra.

## References

1. Qian, Q.; Wu, A. X.; Chi, W. S.; Asinger, P. A.; Lin, S.; Hypsher, A.; Smith, Z. P. Mixed-Matrix Membranes Formed from Imide-Functionalized UiO-66-NH<sub>2</sub> for Improved Interfacial Compatibility. *ACS Appl. Mater. Interfaces* **2019**, *11*, 31257-31269.
2. Hintz, H.; Wuttke, S. Postsynthetic modification of an amino-tagged MOF using peptide coupling reagents: a comparative study. *Chem. Commun.* **2014**, *50*, 11472-11475.
3. Lu, X.; Jiang, J.; Sun, K.; Wang, J.; Zhang, Y. Influence of the pore structure and surface chemical properties of activated carbon on the adsorption of mercury from aqueous solutions. *Marine Pollution Bulletin* **2014**, *78*, 69-76.
4. Fardmousavi, O.; Faghihian, H. Thiol-functionalized hierarchical zeolite nanocomposite for adsorption of Hg<sup>2+</sup> from aqueous solutions. *Comptes Rendus Chimie* **2014**, *17*, 1203-1211.
5. Arias Arias, F. E.; Beneduci, A.; Chidichimo, F.; Furia, E.; Straface, S. Study of the adsorption of mercury (II) on lignocellulosic materials under static and dynamic conditions. *Chemosphere (Oxford)* **2017**, *180*, 11-23.
6. Najafi, M.; Rostamian, R.; Rafati, A. A. Chemically modified silica gel with thiol group as an adsorbent for retention of some toxic soft metal ions from water and industrial effluent. *Chem. Eng. J.* **2011**, *168*, 426-432.
7. Rostamian, R.; Najafi, M.; Rafati, A. A. Synthesis and characterization of thiol-functionalized silica nano hollow sphere as a novel adsorbent for removal of poisonous heavy metal ions from water: Kinetics, isotherms and error analysis. *Chem. Eng. J.* **2011**, *171*, 1004-1011.
8. Fu, L.; Wang, S.; Lin, G.; Zhang, L.; Liu, Q.; Fang, J.; Wei, C.; Liu, G. Post-functionalization of UiO-66-NH<sub>2</sub> by 2,5-Dimercapto-1,3,4-thiadiazole for the high efficient removal of Hg(II) in water. *Journal of Hazardous Materials* **2019**, *368*, 42-51.
9. Feng, L.; Zeng, T.; Hou, H. Post-functionalized metal-organic framework for effective and selective removal of Hg(II) in aqueous media. *Microporous and Mesoporous Materials* **2021**, *328*.
10. Zhao, M.; Huang, Z.; Wang, S.; Zhang, L.; Zhou, Y. Design of l-Cysteine Functionalized UiO-66 MOFs for Selective Adsorption of Hg(II) in Aqueous Medium. *ACS Appl. Mater. Interfaces* **2019**, *11*, 46973.
11. Liu, F.; Xiong, W.; Feng, X.; Cheng, G.; Shi, L.; Chen, D.; Zhang, Y. Highly recyclable cysteamine-modified acid-resistant MOFs for enhancing Hg (II) removal from water. *Environ. Technol.* **2020**, *41*, 3094-3104.
12. Ding, L.; Luo, X.; Shao, P.; Yang, J.; Sun, D. Thiol-Functionalized Zr-Based Metal-Organic Framework for Capture of Hg(II) through a Proton Exchange Reaction. *ACS Sustainable Chem. Eng.* **2018**, *6*, 8494-8502.

13. He, Y.; Hou, Y.; Wong, Y.; Xiao, R.; Li, M.; Hao, Z.; Huang, J.; Wang, L.; Zeller, M.; He, J.; Xu, Z. Improving stability against desolvation and mercury removal performance of Zr(IV)-carboxylate frameworks by using bulky sulfur functions. *J. Mater. Chem. A* **2018**, *6*, 1648-1654.
14. Zhang, L.; Wang, J.; Wang, H.; Zhang, W.; Zhu, W.; Du, T.; Ni, Y.; Xie, X.; Sun, J.; Wang, J. Rational design of smart adsorbent equipped with a sensitive indicator via ligand exchange: A hierarchical porous mixed-ligand MOF for simultaneous removal and detection of Hg<sup>2+</sup>. *Nano Res* **2021**, *14*, 1523-1532.
15. Lin, D.; Liu, X.; Huang, R.; Qi, W.; Su, R.; He, Z. One-pot synthesis of mercapto functionalized Zr-MOFs for the enhanced removal of Hg<sup>2+</sup> ions from water. *Chem. Commun.* **2019**, *55*, 6775-6778.
16. Wu, J.; Zhou, J.; Zhang, S.; Alsaedi, A.; Hayat, T.; Li, J.; Song, Y. Efficient removal of metal contaminants by EDTA modified MOF from aqueous solutions. *J. Colloid Interface Sci.* **2019**, *555*, 403-412.
17. Li, M.; Wong, Y.; Lum, T.; Sze-Yin Leung, K.; Lam, P. K. S.; Xu, Z. Dense thiol arrays for metal-organic frameworks: boiling water stability, Hg removal beyond 2 ppb and facile crosslinking. *J. Mater. Chem. A* **2018**, *6*, 14566-14570.
18. Hu, Y.; Wang, S.; Zhang, L.; Yang, F. Selective removal of Hg(II) by UiO-66-NH<sub>2</sub> modified by 4-quinolinecarboxaldehyde: from experiment to mechanism. *Environmental Science and Pollution Research* **2023**, *30*, 2283-2297.
19. Awad, F. S.; Bakry, A. M.; Ibrahim, A. A.; Lin, A.; El-Shall, M. S. Thiol- and Amine-Incorporated UiO-66-NH<sub>2</sub> as an Efficient Adsorbent for the Removal of Mercury(II) and Phosphate Ions from Aqueous Solutions. *Ind. Eng. Chem. Res.* **2021**, *60*, 12675.
20. Lin, G.; Zeng, B.; Liu, X.; Li, J.; Zhang, B.; Zhang, L. Enhanced performance of functionalized MOF adsorbents for efficient removal of anthropogenic Hg(II) from water. *J. Clean. Prod.* **2022**, *381*, 134766.